

# Mechanical Property of a TIM-Barrel Protein

Nobuo Kobayashi,<sup>1</sup> Takahisa Yamato,<sup>2</sup> and Nobuhiro Go<sup>1\*</sup>

<sup>1</sup>Department of Chemistry, Graduate School of Science, Kyoto University, Kyoto, Japan

<sup>2</sup>Department of Material System Engineering, Faculty of Technology, Tokyo University of Agriculture and Technology, Koganei, Tokyo, Japan

**ABSTRACT** The mechanical response of a TIM-barrel protein to an applied pressure has been studied. We generated structures under an applied pressure by assuming the volume change to be a linear function of normal mode variables. By Delaunay tessellation, the space occupied by protein atoms is divided uniquely into tetrahedra, whose four vertices correspond to atomic positions. Based on the atoms that define them, the resulting Delaunay tetrahedra are classified as belonging to various secondary structures in the protein. The compressibility of various regions identified with respect to secondary structural elements in this protein is obtained from volume changes of respective regions in two structures with and without an applied pressure. We found that the  $\beta$  barrel region located at the core of the protein is quite soft. The interior of the  $\beta$  barrel, occupied by side chains of  $\beta$  strands, is the softest. The helix, strand, and loop segments themselves are extremely rigid, while the regions existing between these secondary structural elements are soft. These results suggest that the regions between secondary structural elements play an important role in protein dynamics. Another aspect of tetrahedra, referred to as *bond distance*, is introduced to account for rigidities of the tetrahedra. Bond distance is a measure of separation of the atoms of a tetrahedron in terms of number of bonds along the polypeptide chain or side chains. Tetrahedra with longer bond distances are found to be softer on average. From this behavior, we derive a simple empirical equation, which well describes the compressibilities of various regions. *Proteins* 28:109–116, 1997. © 1997 Wiley-Liss, Inc.

**Key words:** normal mode analysis; Delaunay tessellation; bond distance; compressibility; volume fluctuation

## INTRODUCTION

Protein tertiary structures are made up of such secondary structural elements as  $\alpha$  helices,  $\beta$  strands, and loops, which are mutually well packed to form three-dimensional structures. Having such struc-

tures, protein interior is expected to be mechanically heterogeneous with relatively rigid and soft parts. In this paper we are interested in which parts of a protein are soft and which parts are rigid.

The elucidation of mechanical construction of proteins is interesting from a number of points of view, as follows:

1. There are classes of proteins whose functions are to exert force on molecules interacting with them, for example, kinesin or myosin. Such forces must be balanced by forces induced in an interior of a protein. Therefore, the mechanical properties are directly related to functions.
2. Pressure is an important thermodynamic parameter, along with temperature, in studying the physicochemical properties of protein. Response of a protein conformation to an applied pressure is governed by compressibility of various parts of a molecule.
3. Compressibility is related to volume fluctuation. Various conformational fluctuations, often leading to volume fluctuation, are supposed to play a role in many types of protein functions.

Theoretical study of mechanical construction of proteins was first carried out by Yamato et al.<sup>1</sup> on deoxymyoglobin, which is composed mainly of  $\alpha$  helices. They studied compressibilities of  $\alpha$  helices and regions between  $\alpha$  helices and found that  $\alpha$  helices are quite rigid, but regions between  $\alpha$  helices are very soft. This fact explains experimental observations<sup>2,3</sup> that helix-rich proteins generally show high compressibilities.

The purpose of this paper is to extend the above study to a protein that has a  $\beta$  sheet—triosephosphate isomerase (TIM). An eight-stranded parallel  $\beta$  sheet surrounded by eight  $\alpha$  helices in this protein takes a barrel-like form, called TIM barrel, in a highly symmetric arrangement, which is found in many proteins of known structures. The interior of the  $\beta$  barrel forms a hydrophobic core.

\*Correspondence to: Nobuhiro Go, Department of Chemistry, Graduate school of Science, Kyoto University, Kitashirakawa-Oiwakecho, Kyoto 606-01, Japan.

Received 14 May 1996; Accepted 24 October 1996

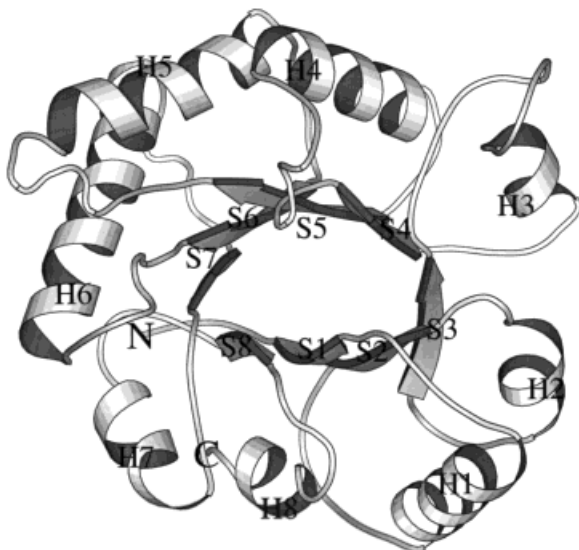


Fig. 1. Ribbon diagram<sup>18</sup> of triosephosphate isomerase (TIM). "N" and "C" indicate the position of N and C termini. Strands and helices are indicated by "S" and "H".

We define various regions of the molecule with respect to secondary structural elements by employing the idea of Delaunay tessellation.<sup>4</sup> The computational geometry methods of Delaunay and Voronoi tessellations,<sup>5</sup> which are mathematically dual to each other, have been applied to study various geometrical properties of protein structures.<sup>6-8</sup> In this paper we carry out Delaunay tessellation to divide the space occupied by protein atoms into tetrahedra, with all four vertices at atomic positions. The resulting tetrahedra are classified according to secondary structural elements to which the four corner atoms belong. Compressibilities of various regions of this protein are deduced by calculating changes of volume caused by an applied pressure.

## METHODS

### Molecule Studied

TIM is studied as a typical TIM-barrel protein. The x-ray coordinates of this protein are taken from 3TIM<sup>9</sup> in Protein Data Bank (PDB).<sup>10</sup> The structure is shown in Figure 1 by a ribbon diagram. This protein exists usually as a dimer consisting of two identical monomers, each of which has 250 amino acid residues. This number of residues is quite large for carrying out even our calculations which work in dihedral angle space. (This molecule has the smallest number of residues among the molecules having TIM-barrel structures and deposited in the PDB.) All atoms including generated hydrogen atoms are treated explicitly. Each monomer has 3911 atoms and 1441 dihedral angles.

We carry out all calculations for the monomeric state of this protein. In other words, we neglect all intermonomer interactions existing in the dimeric

state. Monomers are in contact with each other at one loop region, called the interface loop. Because we are mainly interested in the mechanical properties of the  $\beta$  barrel region, which is in the core of each monomer, the neglect of intermonomer interactions in our calculation is expected not to influence results significantly.

### Linear Approximation of Volume Change

The mathematical formulation used in this paper has been largely developed in our earlier paper,<sup>1</sup> and is described here only briefly.

Energy minimization is done by employing the ECEPP energy function.<sup>11</sup> Normal mode analysis describes the dynamics of a molecule as a linear sum of independent collective motions, called normal modes. For such a description to be possible, the conformational energy change  $\Delta E$  from that of a minimum-energy conformation must be given by

$$\Delta E = \frac{1}{2} \sum_i \omega_i^2 \sigma_i^2, \quad (1)$$

where  $\omega_i$  is the angular frequency of  $i$ th normal mode and  $\sigma_i$  is the  $i$ th normal mode variable. The thermal average of fluctuation in each normal mode variable is given by

$$\langle \sigma_i \sigma_j \rangle = \frac{k_B T}{\omega_i^2} \delta_{ij}, \quad (2)$$

where  $k_B$  is the Boltzmann constant, and  $T$  is the absolute temperature.

In the spirit of normal mode analysis, we approximate the volume change associated with conformational fluctuation as a linear function of normal mode variables

$$\Delta V = \sum_i v_i \sigma_i, \quad (3)$$

where  $v_i$  is the derivative of volume with respect to  $i$ th normal mode variable  $\sigma_i$  at the minimum-energy conformation. In this paper we use the excluded volume<sup>6</sup>—the volume enclosed by the solvent accessible surface—as the molecular volume.

As was shown in our earlier paper,<sup>1</sup> the shift of the average value of  $i$ th normal mode variable under a pressure  $P$  is given by

$$\sigma_i(P) = -P \frac{v_i}{\omega_i^2}. \quad (4)$$

Once values of normal mode variables are known, a set of dihedral angles, and hence a set of cartesian coordinates of the conformation under the applied pressure, can be calculated. By calculating molecular volumes explicitly for conformations with and

without applied pressure, volume compression can be obtained, from which we obtain a compressibility.

Compressibility can also be obtained from the magnitude of volume fluctuation under no applied pressure. Within the linear approximation of volume change, the volume fluctuation  $\langle(\Delta V)^2\rangle$  (and hence the isothermal compressibility  $\beta_T$ ) can be calculated analytically as<sup>12</sup>

$$\begin{aligned}\langle(\Delta V)^2\rangle &= \left\langle \left( \sum_i v_i \sigma_i \right)^2 \right\rangle \\ &= k_B T \sum_i \left( \frac{v_i}{\omega_i} \right)^2,\end{aligned}\quad (5)$$

and

$$\begin{aligned}\beta_T &= \frac{1}{k_B T V_0} \langle(\Delta V)^2\rangle, \\ &= \frac{1}{V_0} \sum_i \left( \frac{v_i}{\omega_i} \right)^2,\end{aligned}\quad (6)$$

where  $V_0$  is the volume of the molecule at the minimum-energy conformation.

### Detailed Analysis of Conformational Deformation

Following the treatment in our earlier paper,<sup>1</sup> we carry out a detailed analysis of conformational deformation from the minimum-energy conformation to that at a pressure  $P$  as follows.

At first we divide the space occupied by protein atoms into tetrahedra whose vertices are at neighboring atoms. The method of division employed in our earlier paper<sup>1</sup> was slightly unsatisfactory in the sense that a very small fraction of the space was not included in any tetrahedra. This problem has been solved by Yamato<sup>4</sup> with the use of the Delaunay tessellation.<sup>13</sup> This method is mathematically dual to the Voronoi tessellation in the sense that Delaunay tetrahedra are obtained by replacing each plane surface of the Voronoi polyhedra by a straight-line segment connecting a pair of atoms. Because Voronoi tessellation uniquely divides the protein space into polyhedra, its mathematically dual method, the Delaunay tessellation also uniquely divides the space occupied by the protein atoms. The Delaunay tetrahedra correspond to the space shared by neighboring atoms. We used the efficient algorithm of Delaunay tessellation developed by Tanemura et al.<sup>13</sup> All atoms except hydrogen atoms are treated explicitly in the Delaunay tessellation.

### Classification of the Delaunay Tetrahedra According to the Structural Units

The tetrahedra are classified according to their location with respect to various secondary structural elements in the protein. As secondary structural

elements, we focus our attention on the eight  $\alpha$  helices and the eight  $\beta$  strands. We refer to the eight  $\beta$  strands collectively as  $\beta$  barrel, and to the other regions as loops. There are 15 loops connecting  $\alpha$  helices and  $\beta$  strands, plus N and C termini. Main-chain and side-chain atoms are regarded as belonging to the same structural elements, defined by the main chain. Thus, each atom belongs to either helix (H), barrel (B), or loops (L). We classify the tetrahedra into "helix," "barrel," "loop," "helix-barrel," "helix-loop," "barrel-loop," and "helix-barrel-loop," depending on the types of its constituent atoms. The classification is done as follows. If the types of four atoms of a tetrahedron consist, for example, of only H, of H and B, or of H, B, and L, then the tetrahedron is classified into "helix," "helix-barrel," or "helix-barrel-loop," respectively. "Helix," "barrel," and "loop" are further classified into "intrahelix" and "interhelix," and so on. If four atoms of a "helix" tetrahedron belong to the same helix, then the tetrahedron is classified into "intrahelix." Otherwise, it is classified into "interhelix."

The  $\beta$  barrel is further classified into main-chain "sheet" region, "interior" region inside the barrel, and "exterior" region outside the barrel. This classification is made as follows: Each of four atoms in a  $\beta$  barrel tetrahedron is classified into three types: backbone atom, inside side-chain atom, and outside side-chain atom. If three or four atoms of a tetrahedron belong to backbone, inside or outside, then the tetrahedron is classified as "sheet," "interior," or "exterior," respectively. If two belong to backbone and the other two to inside or outside, then the tetrahedron is classified as "interior" or "exterior," respectively. There were no other cases.

## RESULTS

### Normal Mode Analysis

Figure 2 shows the distribution of normal mode frequencies in this molecule. The total number of normal modes is of course the same as the number of independent dihedral angles. It is remarkable that the frequency density distribution is very similar to those of smaller proteins. The lowest and highest frequencies are  $3.05\text{ cm}^{-1}$  and  $1005.4\text{ cm}^{-1}$ , respectively. There are 1105 modes with frequencies below  $200\text{ cm}^{-1}$ , which account for 76.7% of all modes in this calculation.

Figure 3 shows the atomic displacement vectors of C $\alpha$  atoms for three of the very-low frequency modes. In the lowest frequency mode (Fig. 3a), a large motion, localized on the interface loop in  $\beta/\alpha$  fragment number 3, is observed. This loop is in contact with the other subunit in the dimeric state, but, as stated above, we neglect this contact in this calculation. Therefore, this localized motion occurs only in the monomeric state. In the second lowest frequency mode (Fig. 3b), a nonlocalized collective motion is observed. This motion is like a "hinge-bending" mo-

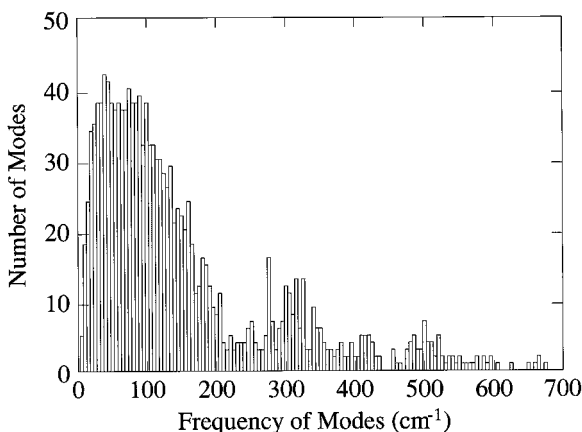


Fig. 2. Histogram of frequencies of normal modes of TIM calculated in the dihedral angle space. Number of normal modes in each interval of  $5 \text{ cm}^{-1}$  is shown. There are 14 more modes in the range above  $700 \text{ cm}^{-1}$ .

tion between two structural units, one consisting of  $\beta/\alpha$  fragments 1, 2, 7, and 8, and the other, of fragments 5 and 6. The active site is on the loop between sixth  $\beta$  strand and  $\alpha$  helix. Therefore this motion is expected to play an important role in the function of this protein. In the fourth lowest frequency mode (Fig. 3c),  $\beta/\alpha$  fragments 4 and 6 are bending. This motion is also expected to play an important role in the function.

### Volume Fluctuation

From Equation (5) we see that the contribution from each normal mode to volume fluctuation is proportional to  $k_B T (v_j/\omega_j)^2$ . In Figure 4 this quantity is plotted for modes with frequencies lower than  $50 \text{ cm}^{-1}$  for  $T = 300 \text{ K}$ . (The contributions from modes with frequency higher than  $50 \text{ cm}^{-1}$  are small.) The maximum contribution of  $1922 \text{ \AA}^6$  comes from mode 2. It is clear that very low frequency modes make dominant contributions. Root-mean-square (rms) volume fluctuation  $\langle(\Delta V)^2\rangle^{1/2}$  is  $155.48 \text{ \AA}^3$ . The rms volume fluctuation, the excluded volume,<sup>14</sup> and the isothermal compressibility obtained from Equation (6) are given in Table I. The magnitude of the compressibility is in the range of experimental values for various globular proteins.

### Conformational Deformation Due To an Applied Pressure

The equilibrium conformation under an applied pressure of 1,000 atm is generated from the shift of normal mode variables given by Equation (4). The structure of the minimum-energy conformation and displacement vectors of  $C_\alpha$  atoms are shown in Figure 5. Although this molecule's arrangement of secondary structures is very symmetric, the magnitudes of atomic displacements under pressure are not uniform, but are large in a region containing

both the N and C termini. These large displacements may be attributed to the discontinuity of the polypeptide chain in this region. The change of the excluded volume by the applied pressure and the compressibility calculated therefrom are also given in Table I.

Next we carry out Delaunay tessellation for the two conformations. The numbers of tetrahedra for the minimum-energy conformation and the conformation under pressure are 10,925 and 10,935, respectively. The total volumes of the Delaunay tetrahedra and the compressibility calculated from the volume change are also given in Table I. Of the above tetrahedra, about 90% (9,842) consist of the same set of atoms and therefore are common to the two conformations. The total volumes of these tetrahedra and the compressibility calculated therefrom are also given in Table I.

The four different calculated compressibilities, that is—(1) obtained from the volume fluctuation ( $11.9 \times 10^{-12} \text{ cm}^2/\text{dyn}$ ), (2) calculated from the compression of excluded volume ( $14.8 \times 10^{-12} \text{ cm}^2/\text{dyn}$ ), and (3) and (4) calculated from compression of the volume of all the tetrahedra ( $17.5 \times 10^{-12} \text{ cm}^2/\text{dyn}$ ) and the common tetrahedra ( $17.1 \times 10^{-12} \text{ cm}^2/\text{dyn}$ ) are not identical. The difference between (1) and (2) is due to the linear approximation of volume change. Such a difference was also observed in the case of myoglobin.<sup>1</sup> We reported that the linearity of volume change is approximately valid with a possible underestimation of 20%. The difference in this study is also likely to be due to this underestimation. The difference between (2) on the one hand, and (3) and (4) on the other, is complicated. Since the tetrahedra form the molecule's core, the difference should be attributed to the volume change of the surface region. This then implies that the surface region is more rigid than the interior region. The volume of the surface region is  $21,007 \text{ \AA}^3$ , its compression under the pressure is  $237 \text{ \AA}^3$ , and the compressibility calculated therefrom is  $11.1 \times 10^{-12} \text{ cm}^2/\text{dyn}$ . This point is discussed in a later section.

### Mechanical Properties of Different Types of Structural Units

Next we classify the common tetrahedra according to their location with respect to various secondary structural elements. The sum of volumes of tetrahedra classified into each type is calculated for two conformations, one under no pressure, the other under an applied pressure of 1,000 atm, and from the differences, isothermal compressibilities are evaluated. The results, which are summarized in Table II, indicate that the "intraunit" regions are extremely rigid and the "interunit" regions are soft except for the "interhelix" region. The regions between different secondary structural elements are soft except for the "helix-loop" region. The " $\beta$  barrel interior" is found to be strikingly soft.

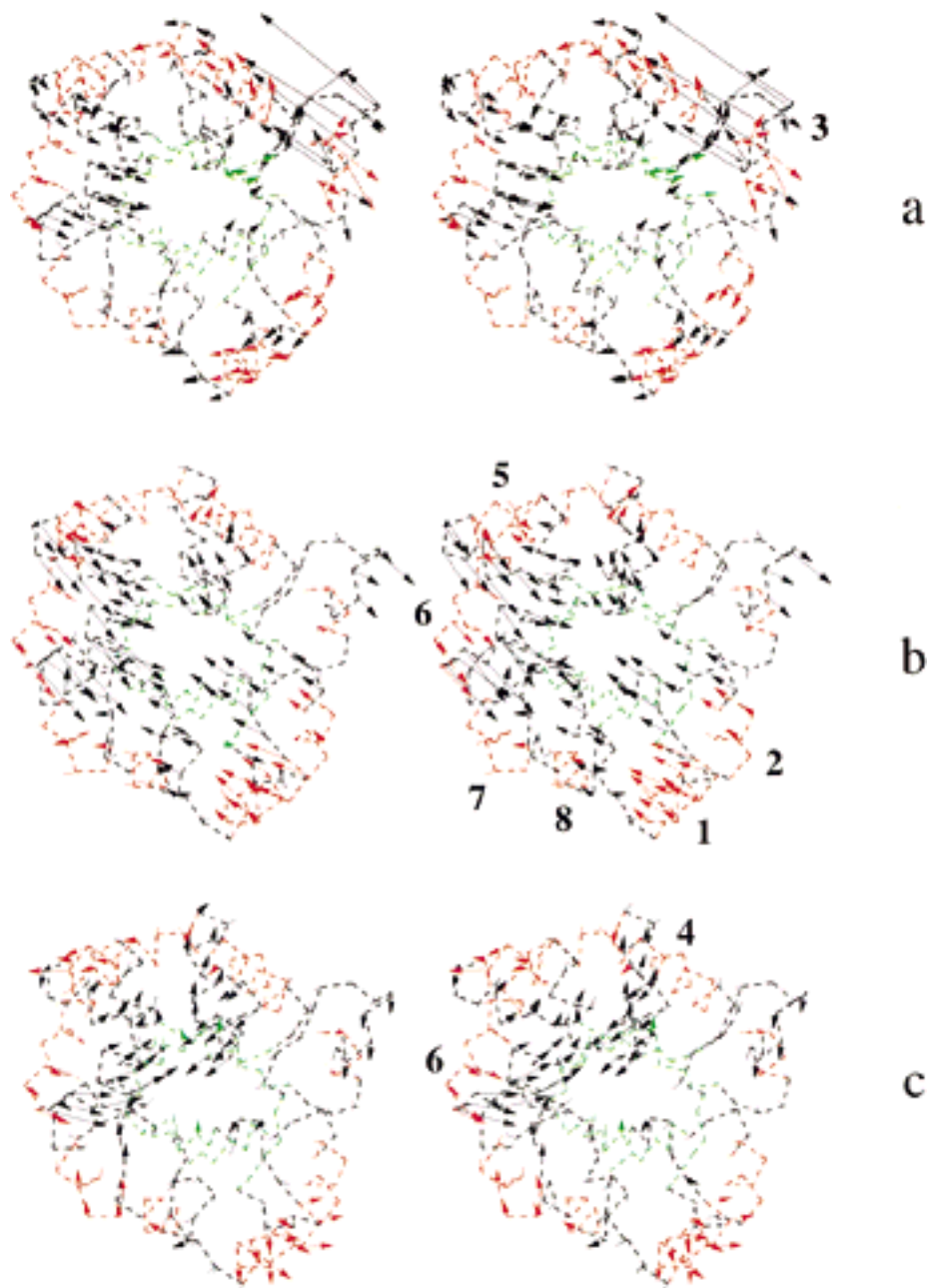


Fig. 3. Stereo drawing of atomic displacement vectors. **a:** The lowest frequency normal mode with  $3.05 \text{ cm}^{-1}$ . **b:** The 2nd lowest frequency mode with  $3.35 \text{ cm}^{-1}$ . **c:** The 4th lowest frequency mode with  $4.62 \text{ cm}^{-1}$ . Broken lines indicate traces of  $C\alpha$  atoms, and arrows indicate atomic displacement vectors. Green regions

are the residues whose secondary structures are  $\beta$  strands; red regions,  $\alpha$  helices; and black regions, neither of them.  $\beta/\alpha$  fragment numbers are also indicated only for those fragments discussed in the text. All vectors are magnified 20 times the thermal root-mean-square amplitude.

### Classification of Tetrahedra According to Bond Distance

We have shown that the “intraunit” regions are very rigid and the other regions, especially the “ $\beta$  barrel interior,” are soft. We want to find a more unified view to explain these findings. For this purpose, we classify tetrahedra according to *distances between constituent atoms through covalent*

*bonds*. It is expected that the atoms of the intraunit tetrahedra have shorter distances through covalent bonds than those of other tetrahedra. A bond distance between a pair of atoms is defined as the number of covalent bonds that exist in the shortest route between them, and a bond distance of a tetrahedron is defined as the sum of bond distances for all possible six pairs of atoms out of the four

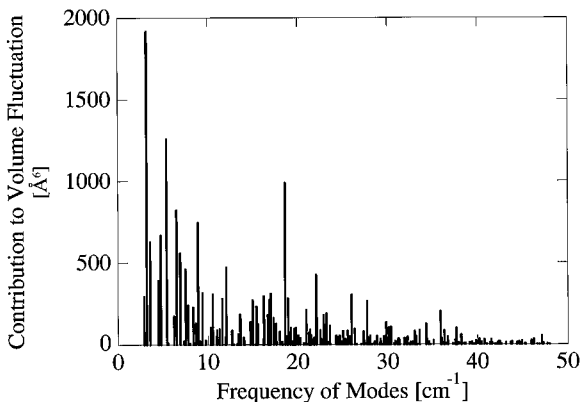


Fig. 4. Contribution to mean-square volume fluctuation from each normal mode in the frequency range below 50  $\text{cm}^{-1}$ .

**TABLE I. The Isothermal Compressibilities Obtained from the Volume Fluctuation and the Volume Compression\***

	$\beta_T^{fluc} \times 10^{12}$ ( $\text{cm}^2/\text{dyn}$ )	$V_0$ ( $\text{\AA}^3$ )	$((\Delta V)^2)^{1/2}$ ( $\text{\AA}^3$ )
Whole molecule	11.9	48908	155
	$\beta_T^{comp} \times 10^{12}$ ( $\text{cm}^2/\text{dyn}$ )	$V_0$ ( $\text{\AA}^3$ )	$\Delta V$ ( $\text{\AA}^3$ )
Whole molecule	14.8	48908	731
Region occupied by all the tetrahedra	17.5	27900	494
Region occupied by the common tetrahedra <sup>†</sup>	17.1	23826	412

\*The volume of the minimum-energy conformation,  $V_0$ ; the root-mean-square volume fluctuation,  $((\Delta V)^2)^{1/2}$ ; the volume compression  $\Delta V = V_0 - V_{1000}$ , where  $V_{1000}$  is the volume under the pressure of 1,000 atm; the isothermal compressibility obtained from volume compression,  $\beta_T^{comp}$ ; and the isothermal compressibility obtained from volume fluctuation,  $\beta_T^{fluc}$ .

<sup>†</sup>The region occupied by those tetrahedra common in the two conformations, the minimum-energy conformation and the conformation under the pressure of 1,000 atm.

atoms in the tetrahedron. The bond distances of tetrahedra vary from 9 to 2930. Figure 6 shows the distribution of bond distances and the compressibility of tetrahedra averaged in each interval, clearly indicating the statistical relation between the bond distances and the compressibility. From this behavior, we classify the tetrahedra into three types:

- Class I: those with short bond distances, from 9 to 150 (average compressibility,  $5.32 \times 10^{-12} \text{ cm}^2/\text{dyn}$ )
- Class II: those with intermediate bond distances, from 150 to 700 (average compressibility,  $17.2 \times 10^{-12} \text{ cm}^2/\text{dyn}$ )
- Class III: long bond distances, above 700 (average compressibility,  $54.9 \times 10^{-12} \text{ cm}^2/\text{dyn}$ )

Bond distances of all “intraunit” tetrahedra are below 150, and those of all “interunit” tetrahedra are above 150. Thus, all “intraunit” tetrahedra and no “interunit” tetrahedra are in class I.

The volume ratios of these classes are also shown in Table II for each structural region. In order to describe the compressibility from these volume ratios, we introduce an empirical equation:

$$\hat{\beta}_T = \beta_I \rho_I + \beta_{II} \rho_{II} + \beta_{III} \rho_{III}, \quad (7)$$

where  $\hat{\beta}_T$  is the estimated compressibility,  $\rho_I$ ,  $\rho_{II}$ , and  $\rho_{III}$  are the volume ratios, and  $\beta_I$ ,  $\beta_{II}$ , and  $\beta_{III}$  are the above average compressibilities of classes I, II, and III, respectively. The estimated compressibilities and the errors of the estimation are also shown in Table II. We see that the compressibility of each region can be estimated quite well by the simple empirical Equation (7), with only three parameters. The estimation is less satisfactory for the “helix–barrel–loop” region. In this region, the average volume of tetrahedra is much larger than those in the other regions. This large volume, which implies large packing defects, make this region softer than estimated.

## DISCUSSION

In our previous study of compressibility on deoxy-myoglobin,<sup>1</sup> it was observed that the intrahelix was rigid and the interhelix was soft. The average compressibilities of tetrahedra were  $0.60 \times 10^{-12} \text{ cm}^2/\text{dyn}$  in the intrahelix and  $8.94 \times 10^{-12} \text{ cm}^2/\text{dyn}$  in the interhelix. These values are somewhat smaller than the corresponding values in Table II. However, these differences are mainly due to different definitions of compressibilities. In the present paper the average compressibility is calculated with weight equal to the volume of respective tetrahedron, while in the previous paper the average compressibility is calculated without volume weight. Since a tetrahedron with larger volume tends to be softer, the volume-weighted average compressibility should be larger. In fact, unweighted compressibilities of intrahelix and interhelix tetrahedra in TIM are  $0.98 \times 10^{-12} \text{ cm}^2/\text{dyn}$  and  $12.2 \times 10^{-12} \text{ cm}^2/\text{dyn}$ , respectively. These values, smaller than the values in Table II, are similar to the values obtained for deoxymyoglobin. Therefore we may be able to say that compressibilities of intrahelix and interhelix regions are generally in the range of  $1 \times 10^{-12} \text{ cm}^2/\text{dyn}$  and  $10 \times 10^{-12} \text{ cm}^2/\text{dyn}$ , respectively.

We have obtained results showing that the protein interior is mechanically very heterogeneous, various regions having compressibilities from  $2 \times 10^{-12} \text{ cm}^2/\text{dyn}$  to  $40 \times 10^{-12} \text{ cm}^2/\text{dyn}$ . These values are to be compared with the isothermal compressibility of water ( $45 \times 10^{-12} \text{ cm}^2/\text{dyn}$ ) and of ice ( $12 \times 10^{-12} \text{ cm}^2/\text{dyn}$ ). Thus, this protein contains both the regions more rigid than ice and the regions as soft as water. From the experimental results,<sup>2,3</sup> the com-

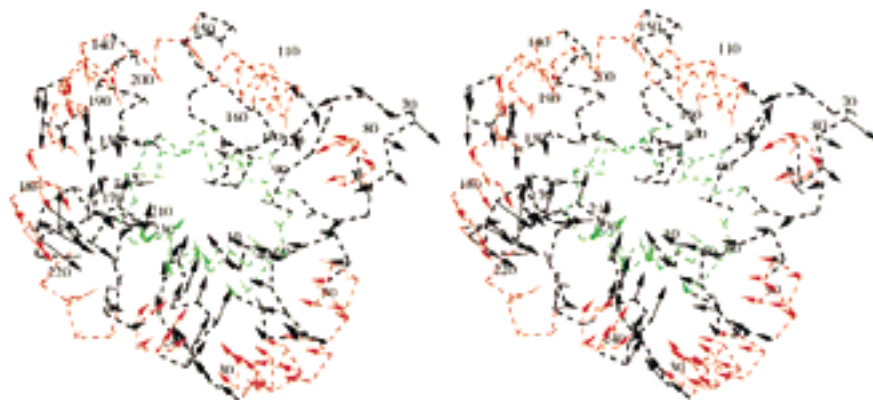


Fig. 5. Stereo drawing of conformational deformation in TIM due to application of 1,000 atm hydrostatic pressure. The dotted line represents the  $C_{\alpha}$  skeleton with the same color code as in

Figure 3, and the arrows represent displacement vectors of  $C_{\alpha}$  atoms, whose magnitude is magnified 10 times. Sequence numbers are also indicated.

**TABLE II. Various Features of Each Type of Structural Regions\***

	Number of tetrahedra	$\beta_T \times 10^{12}$ (cm <sup>2</sup> /dyn)	$V_0$ (Å <sup>3</sup> )	$\bar{V}$ (Å <sup>3</sup> )	Volume ratio (%)			$\hat{\beta}_T \times 10^{12}$ (cm <sup>2</sup> /dyn)	$(\beta_T - \hat{\beta}_T) \times 10^{12}$ (cm <sup>2</sup> /dyn)
					I	II	III		
common <sup>†</sup>	9842	17.1	23826	2.42	0.42	0.45	0.13	17.11	-0.01
intra-helix	1955	2.80	2677	1.37	1.00	0.00	0.00	5.32	-2.52
intra-loop	2415	4.15	3353	1.39	1.00	0.00	0.00	5.32	-1.17
inter-helix	304	14.4	1178	3.88	0.00	0.97	0.03	18.33	-3.93
inter-loop	732	28.4	2796	3.82	0.00	0.70	0.30	28.51	-0.11
helix-barrel	361	21.5	1430	3.96	0.18	0.65	0.16	20.92	0.58
helix-loop	1825	12.5	5685	3.11	0.43	0.46	0.10	15.69	-3.19
barrel-loop	939	28.5	2979	3.17	0.22	0.56	0.22	22.88	5.62
helix-barrel-loop	239	32.7	1363	5.70	0.12	0.78	0.10	19.54	13.16
$\beta$ -barrel	1072	24.3	2366	2.21	0.18	0.57	0.25	24.49	-0.19
sheet <sup>‡</sup>	542	9.16	794	1.47	0.32	0.56	0.10	16.82	-7.66
interior <sup>‡</sup>	331	41.7	1090	3.29	0.06	0.50	0.44	33.08	8.62
exterior <sup>‡</sup>	199	10.2	482	2.42	0.22	0.73	0.05	16.47	-6.27
intra-strand <sup>§</sup>	500	2.04	436	0.87	1.00	0.00	0.00	5.32	-3.28
inter-strand <sup>§</sup>	572	29.4	1930	3.37	0.00	0.69	0.31	28.89	0.51

\*Isothermal compressibility,  $\beta_T$ ; volume of the minimum-energy conformation,  $V_0$ ; average volume of tetrahedron,  $\bar{V}$ ; the compressibility estimated by Eq. (7),  $\hat{\beta}_T$ .

<sup>†</sup>Those tetrahedra common in the two conformation, the minimum-energy conformation and the conformation under the applied pressure.

<sup>‡</sup>The  $\beta$ -barrel region is broken down into sheet, interior and exterior.

<sup>§</sup>The  $\beta$ -barrel region is also broken down into intra-strand and inter-strand.

compressibilities of various globular proteins are found to be in the range of  $10\text{--}20 \times 10^{-12}$  cm<sup>2</sup>/dyn. Compressibilities of both the surface and internal regions of this protein were found within this range, with the internal region slightly softer than the surface region. However, we have seen that strikingly soft regions exist within the interior of this protein. Such very soft regions contribute to make the interior region of this protein softer than the surface region.

We carried out our normal mode analysis for the protein in vacuum. Kidera et al.<sup>15,16</sup> have applied the method of the normal mode refinement of protein x-ray crystallography to human lysozyme, and they found that the magnitude of the internal contribu-

tions to the Debye-Waller factors is quantitatively in good agreement with the theoretical prediction by the normal mode analysis in vacuum. This finding provides justification of the use of vacuum normal mode analysis for the study of mechanical properties of protein interior. Although the surface side chains should become much less mobile in the absence of solvent,<sup>17</sup> such effect is expected to be negligible in the dynamics of the core of protein.

## CONCLUSIONS

We have studied the mechanical properties of a TIM-barrel protein. Our method is based on normal mode analysis and the linear approximation of vol-

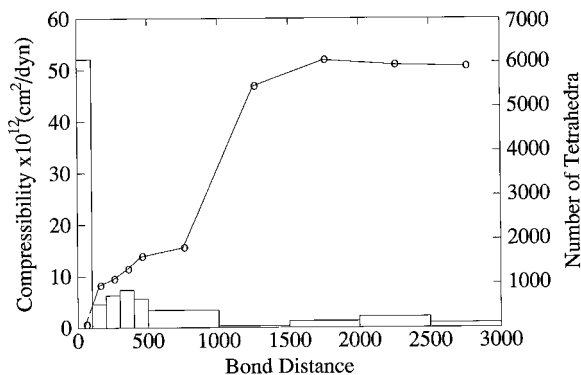


Fig. 6. Histogram of bond distances of all common tetrahedra and the average compressibility of tetrahedra in each interval of 100 bonds below 500 bonds and 500 bonds above 500 bonds.

ume change with respect to changes in the normal mode variables. Delaunay tessellation, which divides the space occupied by a molecule into interatomic spaces, makes it possible to analyze in detail the effects of conformational changes on various interatomic spaces.

The mechanical properties of this protein is found to be very heterogeneous. Among secondary structures,  $\alpha$  helices are found extremely rigid, and  $\beta$  sheets are about three times softer than  $\alpha$  helices. Yet, parts between  $\alpha$  helices and between an  $\alpha$  helix and the  $\beta$  sheet are found to have rigidity roughly in the range of the average value over the whole protein molecule, softer than  $\alpha$  helices and the  $\beta$  sheet. The part packed inside the barrel-shaped  $\beta$  sheet is found to be extremely soft.

The *bond distance*, which is a measure of how far apart the atoms of a tetrahedron are positioned along the polypeptide chain, is a good measure to account for the rigidities of structural regions. Tetrahedra with longer bond distances tend to be softer. From the classification of tetrahedra according to their bond distances, we have been able to introduce a simple empirical equation to estimate the compressibility. If this equation is valid for other proteins, we can estimate the compressibilities of proteins directly from their static three-dimensional structures by simply carrying out Delaunay tessellation and calculating bond distances.

#### ACKNOWLEDGMENTS

We thank Dr. Takahashi for providing graphics program. Computation has been done at the Com-

puter Centers of Kyoto University and of Institute for Molecular Science. This work has been supported by research grants to N.G. from Ministry of Education, Science, and Culture, Japan.

#### REFERENCES

1. Yamato, T., Higo, J., Seno, Y., Go, N. Conformational deformation in deoxymyoglobin by hydrostatic pressure. *Proteins* 16:327-340, 1993.
2. Gekko, K., Noguchi, H. compressibility of globular proteins in water at 25°C. *J. Phys. Chem.* 83:2706-2714, 1979.
3. Gekko, K., Hasegawa, H. Compressibility-structure relationship of globular proteins. *Biochemistry* 25:6563-6571, 1986.
4. Yamato, T. Protein structures and dynamics analyzed by finite elements. Doctoral thesis, Kyoto University.
5. Coxeter, H.S.M. "Introduction to Geometry." New York: Wiley, 1961.
6. Richards, F.M. The interpretation of protein structures: Total volume, group volume distributions and packing density. *J. Mol. Biol.* 82:1-14, 1974.
7. Richards, F.M. Areas, volumes, packing, and protein structure. *Annu. Rev. Biophys. Bioeng.* 6:151-176, 1977.
8. Finney, J.L. Volume occupation, environment and accessibility in proteins: The problem of the protein surface. *J. Mol. Biol.* 96:721-732, 1975.
9. Wierenga, R.K., Noble, M.E.M., Postma, J.P.M., Groendijk, H., Kalk, K.H., Hol, W.G.J., Opperdoes, F.R. The crystal structure of the "open" and the "closed" conformation of the flexible loop of trypanosomal triosephosphate isomerase. *Proteins* 10:33-49, 1991.
10. Bernstein, F.C., Koetzle, T.F., Williams, G.J.B., Meyer, E.F., Brice, M.D., Rodgers, J.R., Kennard, O., Shimanouchi, T., Tasumi, M. The Protein Data Bank: A computer based archival file for macromolecular structures. *J. Mol. Biol.* 122:535-542, 1977.
11. Momany, F.A., McGuire, R.F., Burgess, A.W., Scheraga, H.A. Energy parameters in polypeptide. VII. Geometric parameters, partial atomic charges, nonbonded interactions, hydrogen bond interactions, and intrinsic torsional potentials for the naturally occurring amino acids. *J. Phys. Chem.* 79:2361-2381, 1975.
12. Callen, H.B. The theory of fluctuations. In: "Thermodynamics." New York: Wiley, 1960:267-282.
13. Tanemura, M., Ogawa, T., Ogita, N. A new algorithm for three-dimensional Voronoi tessellation. *J. Comp. Phys.* 51:191-207, 1983.
14. Higo, J., Go, N. Algorithm for rapid calculation of excluded volume of large molecules. *J. Comp. Chem.* 10:376-379, 1989.
15. Kidera, A., Go, N. Normal mode refinement: Crystallographic refinement of protein dynamic structure. I. Theory and test by simulated diffraction data. *J. Mol. Biol.* 225:457-475, 1992.
16. Kidera, A., Go, N. Normal mode refinement: Crystallographic refinement of protein dynamic structure. II. Application to human lysozyme. *J. Mol. Biol.* 225:477-486, 1992.
17. Brooks, C. L. III., Karplus, M. Solvent effects on protein motion and protein effects on solvent motion. *J. Mol. Biol.* 208:159-181, 1989.
18. Kraulis, P.J. MOLSCRIPT: A program to produce both detailed and schematic plots of protein structures. *J. Appl. Crystallogr.* 24:946-950, 1991.